Available online at www.sciencedirect.com
ScienceDirect
Nuclear Instruments and Methods in Physics Research B 255 (2007) 242–246
NIM B
Beam Interactions with Materials & Atoms
www.elsevier.com/locate/nimb

Molecular dynamics study of $B_{18}H_{22}$ cluster implantation into silicon

Luis A. Marqués *, Lourdes Pelaz, Iván Santos

Departamento de Electrónica, Universidad de Valladolid, E.T.S.I. de Telecomunicación, Campus Miguel Delibes s/n, 47011 Valladolid, Spain

Available online 15 December 2006

Abstract

We have carried out molecular dynamics simulations of monatomic B and octadecaborane cluster implantations into Si in order to make a comparative study and determine the advantages and drawbacks of each approach when used to fabricate shallow junctions. We have simulated a total of 1000 cascades of monatomic boron and an equivalent of 56 cascades of octadecaborane in order to have good statistics. We have obtained and analyzed the doping profiles and the amount and morphology of the damage produced within the target. Our simulation results indicate that the use of octadecaborane clusters for the implantation process shows several advantages with respect to monatomic B beams, mainly related to the reduction of channeling and the lower amount of residual damage at the end of range.

PACS: 61.43.Bn; 61.72.Cc; 61.72.Tt; 61.82.Fk

Keywords: Si; B; Octadecaborane; Implantation; Molecular dynamics; Damage generation

1. Introduction

Boron ion implantation has traditionally been used for the fabrication of shallow junctions in MOSFET devices. As technology scales down the energies necessary to fabricate these junctions, monatomic B implantation shows several shortcomings, mainly related to production-throughput and ion-beam high-energy contamination [1]. The implantation of B clusters has been proposed as an alternative to overcome these drawbacks. The use of decaborane ($B_{10}H_{14}$) has been investigated for more than a decade [2–4]. However, this option has not been viable until very recently due to limitations in the source and vapor delivery systems. These problems have been solved by the development of the SemEquip ClusterIon® Source [1], which uses octodecaborane, a molecule with 18 B atoms ($B_{18}H_{22}$) [5]. Recently, the fabrication of MOSFET devices with gate lengths of 60 nm using this equipment has been successfully demonstrated [6].

When fabricating a shallow junction it is important to control not only the dopant profile, but also the amount and type of damage generated during the implantation process. A subsequent anneal is carried out to allow the dopants to diffuse to substitutional sites and so become active, and for the lattice defects to recombine. But this process is highly transient and it is governed by the diffusion and complex interactions between dopants and defects, and especially by their clustering. In particular, interstitial defects produce the so-called transient enhanced diffusion (TED) of B, which alters the junction depth [7]. The amount of TED depends mainly on the net excess of interstitial defects at the end of range (EOR) and their proximity to the target surface [8].

We have carried out molecular dynamics (MD) simulations of monatomic B and octadecaborane cluster implantations into Si in order to make a comparative study and so determine the advantages and drawbacks of each approach. Apart from the doping profiles, we will pay

* Corresponding author. Tel.: +34 983 423 000x5503; fax: +34 983 423 675.
E-mail address: lmarques@ele.uva.es (L.A. Marqués).

0168-583X/$ - see front matter © 2006 Elsevier B.V. All rights reserved.
doi:10.1016/j.nimb.2006.11.038

special attention to the origin, amount and morphology of the damage produced within the target.

2. Simulation details

We have used the Tersoff multi-component potential [9,10] to describe the Si–Si, B–B and Si–B interactions, splined to the Universal potential [11] at short distances to correctly reproduce the high-energy collisions. We have not considered the hydrogen atoms in our simulations, for two reasons: simplicity and because once the octadecaborane molecule is vaporized and ionized it can lose part of its hydrogen atoms, up to 16 of them, before impacting the target surface [1]. Electronic stopping is modeled using a frictional force acting on atoms with energies higher than 10 eV [12]. We solved the classical equations of motion using the 4th order Gear predictor–corrector algorithm [13]. The time-step is variable with the maximum kinetic energy present in the system, but it is always lower than 1 fs. To accelerate the calculations we have used the energy-particle selection (EPS) scheme [14]. It consists of the selective integration of particles as a function of their energy, so low energy particles are integrated less often than high energy particles. The use of this scheme is advantageous mainly at the beginning of the collision cascade, where most of the atoms in the simulation have low energies. The EPS algorithm allows reducing the calculation time by a factor of 3.

In our simulation experiments, we have used Si targets consisting of 32,000 atoms for monatomic B implantations and 600,000 atoms for B_{18} cluster implantations, at an initial temperature of 0 K. These sizes guarantee to contain the full cascades and that once the ion energy is dissipated throughout the target, the increase of temperature is very low to produce damage annealing. Simulation cells are bounded by two (1 0 0) planes in the X direction and by four (1 1 0) planes in the Y and Z directions. Ions are implanted along the X direction with normal incidence on the (1 0 0) Si free surface. The two bottom layers are held fixed and periodic boundary conditions are applied in Y and Z directions. In order to make a statistical study, we have carried out 1000 simulations of monatomic B implantations and an equivalent of 56 of B_{18} cluster implantations. Ion impact points are randomly chosen along the target surface, and in the case of B_{18}, we initially set the B atoms in agreement with the octadecaborane molecule geometry [5], with random rotations around the three axes. Every B atom has an initial energy of 500 eV, a typical value used nowadays for the fabrication of shallow junctions [6].

To identify and characterize the damage resulting from the implantation simulations we have used a method based on the time-average of atom coordinates [15]. Firstly, final configurations are averaged in time for 1000 time-steps. In this way it is possible to eliminate thermal vibrations and consequently to obtain clean configurations. Secondly, the averaged configuration is compared to the perfect lattice: when an atom is closer than 0.7 Å to a lattice site the atom is associated to that site, otherwise it is labeled as "displaced". In the same way, lattice sites with no associated atom are labeled as "empty". And thirdly, displaced atoms and empty lattice sites are grouped following a first neighbor criterion to form defects. The size of the defect is determined by the number of displaced atoms it has, and the type of the defect by the net number of atoms (positive for interstitial-rich defects and negative for vacancy-rich defects).

3. Results and discussion

Fig. 1 shows two snapshots of final system configurations obtained after typical monatomic B and B_{18} cluster implantations. As it is well known, in the monatomic case damage consists of point defects and small disordered zones [10,16]. On average, each 500 eV monatomic B implantation produces only 32 displaced atoms within the target. The mechanisms of damage generation by monatomic B are also fairly well known: the ion produces a cascade where it continuously loses its energy through interactions with the target Si atoms, often generating recoils. The recoil leaves a vacancy behind and generates an interstitial defect where it stops after losing its energy. In the case of B_{18} implantation, final damage structures are completely different. Apart from some point defects, there is a big amorphous zone generated around the cluster impact point. Almost 70% of the implanted B atoms come to rest within this disordered region. A closer look reveals that this amorphous zone is in fact a crater surrounded in the surface by a rim or hump. On average, the number of displaced atoms per implanted B is 108, more than three times the number obtained in monatomic B implantations. In this case the origin of damage is related to the simultaneous deposition of energy carried by the cluster of B atoms on the surface region close to the impact point. The temperature in this zone increases above the melting point causing a crystal-to-liquid transition, similar to the one observed for heavy-ion implantation into Si [16]. When the cascade core cools down due to heat conduction, its temperature drops below melting point and the liquid phase becomes amorphous. Amorphization was also observed in the MD simulations of decaborane implantations into Si described in reference [4], which means that this high-density energy irradiation effect is already present with almost half the number of B atoms in the cluster.

The dopant and damage profiles obtained from the MD simulations of monatomic B and B_{18} cluster implantations are shown in Fig. 2. The boron profiles are very similar, but for two differences. The first one is that there are more dopants close to the target surface in the cluster case, and this is due to B atoms that end up being attached to crater humps. The second difference is a consequence of the channeling of B in the monatomic case. Self-amorphization during cluster implantation results in less B atoms reaching the end-of-range zone in comparison with monatomic B implants. The damage profiles are in turn very different.

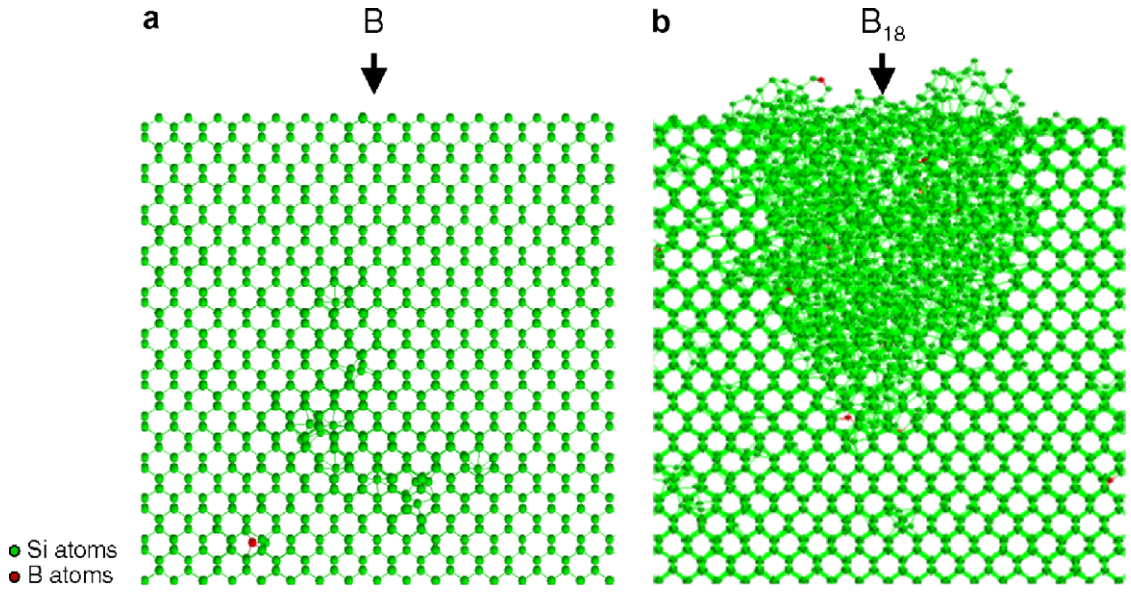

Fig. 1. Lateral snapshots showing the typical damage configurations obtained after implantation of (a) monatomic B, and (b) a B_{18} cluster. Atomic coordinates have been averaged for 1000 time-steps to eliminate thermal vibrations. While in the monatomic case damage is in the form of small defects, cluster implantation produces big amorphous zones.

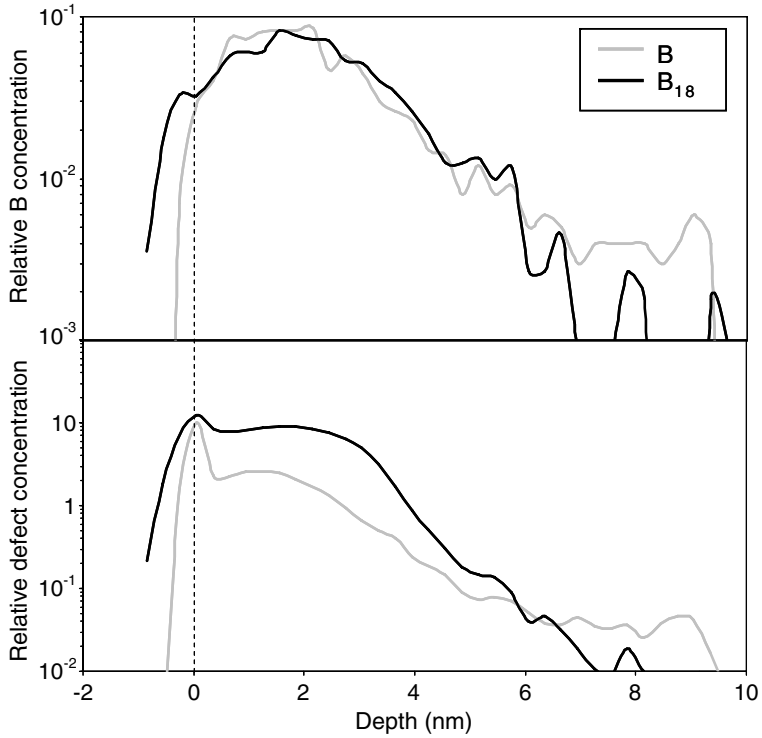

Fig. 2. Dopant and damage profiles obtained for monatomic B and B_{18} cluster implantations. While boron profiles are quite similar, the damage profile obtained after cluster implantations is higher due to big amorphous zones surrounding craters up to a depth of 4 nm. However, the amounts of channeled boron and damage at EOR in the cluster case are lower than in the monatomic case.

In the case of monatomic B, they show a peak at the surface, which corresponds to the formation of small vacancy defects near the ion impact point (where recoils originate). The amount of damage in the cluster case, from the surface up to a depth of 4 nm, is five times higher than in the monatomic case, due to the presence of big amorphous zones surrounding craters. In turn, there is less damage at EOR where channeled B lies.

Fig. 3 shows how displaced atoms created after implantation are distributed in vacancy and interstitial defects as a

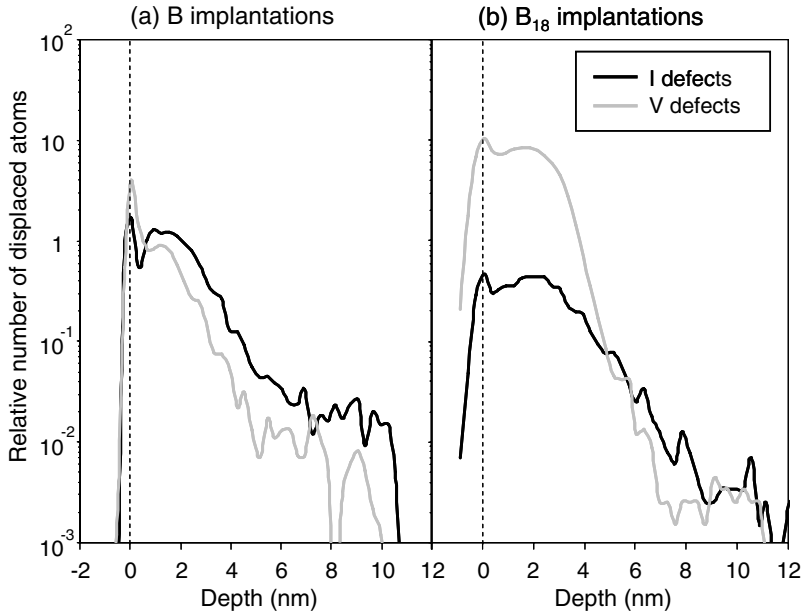

Fig. 3. Distribution of displaced atoms in vacancy and interstitial defects as a function of depth, for (a) monatomic B implantations, and (b) B_{18} cluster implantations. At EOR there is a net excess of interstitial defects in the monatomic case, while in the cluster case they are nearly balanced by vacancy defects.

function of depth. The percentage of occurrence of the different defect types is represented in Table 1. In the case of monatomic B, apart from the surface region where there is an excess of vacancy defects, there is more damage in interstitial defects for all depths. Defects with a high content of vacancies are located in the cascade core, close to the ion impact point on the target surface. This core is surrounded by smaller point defects. It is important to note that at EOR the dominant defects are of interstitial type, single and di-interstitials, which are highly mobile [15] and therefore will cause problems of TED during subsequent thermal treatments. In the case of B_{18} cluster implantations, most of the displaced atoms up to a depth of 4 nm are of vacancy type with high vacancy content (craters). However, the EOR damage is in the form of point defects, and the interstitial and vacancy defect concentration profiles are nearly balanced. This result, and the fact that the amount of residual damage at EOR is lower than in the monatomic case, lead to a smaller negative effect on dopant diffusion.

Table 1
Percentage of displaced atoms in different defect types for monatomic B and B_{18} cluster implantations

Ion	I defects			V defects				
	I	I_2	$I_{>2}$	V	V_2	V_3	V_4	$V_{>4}$
B	89	10	1	36	26	19	9	10
B_{18}	62	36	2	2	2	0	6	90

While in both cases interstitial defects are mainly single- and di-interstitials, vacancy defects show a wider typology. In the case of B_{18} most of displaced atoms are in big vacancy clusters (craters).

4. Conclusions

We have carried out MD simulations of monatomic B and B_{18} cluster implantations into Si in order to make a comparative study. From our simulations, we have analyzed the mechanisms of defect formation, the profiles of implanted B and generated damage, and the morphology of these defects. We have demonstrated that the use of B_{18} clusters to fabricate shallow junctions shows several advantages compared to monatomic B beams. One is the self-amorphization of the target that reduces channeling, so that it is not necessary to have a pre-amorphization step. The formed amorphous layer is very shallow (4 nm thick), so it can be annealed out with a short thermal treatment. The remaining EOR defects are very close to the target surface, which requires lower thermal budgets to their elimination. Besides, the net amount of interstitial defects in this region is lower, and so will be the TED of implanted dopants. Future work will consist of studying the annealing behavior of the amorphous zones generated by cluster implantations.

Acknowledgement

This work has been supported by the Spanish DGI under Project TEC2005-05101 and the JCyL Consejería de Educación y Cultura under Project VA070A05.

References

[1] D. Jacobson, T. Horsky, W. Krull, B. Milgate, Nucl. Instr. and Meth. B 237 (2005) 406.

[2] D. Takeuchi, H. Shimada, J. Matsuo, I. Yamada, Nucl. Instr. and Meth. B 121 (1997) 345.
[3] R. Smith, M. Shaw, R.P. Webb, M.A. Foad, J. Appl. Phys. 83 (1998) 3148.
[4] T. Aoki, J. Matsuo, G. Takaoka, N. Toyoda, I. Yamada, Nucl. Instr. and Meth. B 206 (2003) 855.
[5] P.G. Simpson, W.N. Lipscomb, Proc. Natl. Acad. Sci. 48 (1962) 1490.
[6] Y. Kawasaki et al., Nucl. Instr. and Meth. B 237 (2005) 25.
[7] Y.F. Chong, K.L. Pey, A.T.S. Wee, A. See, L. Chan, Y.F. Lu, W.D. Song, L.H. Chua, Appl. Phys. Lett. 76 (2000) 3197.
[8] M. Aboy, L. Pelaz, L.A. Marqués, L. Enríquez, J. Barbolla, J. Appl. Phys. 94 (2003) 1013.
[9] J. Tersoff, Phys. Rev. B 39 (1989) 5566.
[10] A.M.C. Pérez-Martín, J.J. Jiménez-Rodríguez, J.C. Jiménez-Sáez, Nucl. Instr. and Meth. B 234 (2004) 228.
[11] J.F. Ziegler, J.P. Biersack, U. Littmark, The Stopping and Range of Ions in Solids, Pergamon, New York, 1985.
[12] M. Hedström, H.-P. Cheng, Phys. Rev. B 59 (1999) 10701.
[13] C.W. Gear, Numerical Initial Value Problems in Ordinary Differential Equations, Prentice Hall, Englewood Cliffs, 1971.
[14] L.A. Marqués, J.E. Rubio, M. Jaraíz, L. Enríquez, J. Barbolla, Nucl. Instr. and Meth. B 102 (1995) 7.
[15] L.A. Marqués, L. Pelaz, P. Castrillo, J. Barbolla, Phys. Rev. B 71 (2005) 085204.
[16] M.-J. Caturla, T. Díaz de la Rubia, L.A. Marqués, G.H. Gilmer, Phys. Rev. B 54 (1996) 16683.